24th COBEM - 2017

24th ABCM International Congress of Mechanical Engineering
December 3-8, 2017, Curitiba, PR, Brazil

COBEM-2017-0802
INFLUENCE OF CAVITATION EFFECTS IN JOURNAL BEARINGS ON ROTOR'S DYNAMIC BEHAVIOR

Douglas Jhon Ramos
Gregory Bregion Daniel
School of Mechanical Engineering, UNICAMP, Brazil
djramos@fem.unicamp.br gbdaniel@fem.unicamp.br

Abstract. *The pursuit of mathematical models that correctly describe the dynamic behavior of rotating systems is constant in engineering. One of the models studied is the hydrodynamic lubrication for journal bearings, allowing to evaluation the hydrodynamic forces responsible for shaft's support. This paper presents the inclusion of cavitation effect on oil film, in order to become the lubrication model more reliable and to verify how this effect modifies the rotor's dynamic behavior. The verification was made evaluating the dynamic behavior of the rotor when considered different lubrication condition: Gümbell conditions to solve Reynolds equation and Elrod's universal algorithm. The results obtained in this work show that the influence of the cavitation occurs mainly in critical operational condition when the rotor is near the instability threshold.*

Keywords: *Cavitation in lubrication, Hydrodynamic lubrication, Hydrodynamic bearings)*

1. INTRODUCTION

The development of new technologies has brought with it the need to develop and improve its constituent elements. An example of these elements are the hydrodynamic bearings, widely applied in rotary machines. The lubricating fluid separating the surfaces in relative motion allows the support of large loads at high speeds, as well as reducing the friction from bearing surfaces and avoiding the metal-to-metal contact. Such characteristics make this component widely used in industry, explaining several studies and research involving its dynamic behavior and its interaction with the components of the rotating system.

The importance of using more reliable models in the study of bearings occurs due to to the need to predict the behavior of these components in the rotating system. Understanding the behavior of hydrodynamic bearing in the rotor and associating it with possible operating faults is extremely relevant since the bearings can significantly influence the system response and the faults in this component can be critical and detrimental to the rotating system.

According to Dowson and Taylor (1979), the main points that characterize the fault of a hydrodynamic bearing are lubricating fluid contamination, overheating, metal-to-metal contact, distortions or imperfections in the set and cavitation. By ensuring good control in the assembly, as well as good operating conditions of hydraulic and mechanical systems, it is possible to mitigate or minimize the effects for the vast majority of failures except for the cavitation condition.

Thus, several researchers turned their attention to the phenomenon of cavitation in bearings, seeking to find models that correctly described the effects of this phenomenon. Floberg (1973), Jakobsson and Floberg (1957), Olsson (1965) and Floberg (1974), working independently, were responsible for developing the so-called "Cavitation Theory of JFO", that includes the cavitation effect in the lubricant analysis of the bearing.

The inclusion of cavitation effects in the model of the bearing allows verifying the main changes in the pressure distribution and hydrodynamic forces in relation to the model that does not consider these effects. Knowing these differences, for the static case (rotor locus) and for the dynamic case (rotor orbits), can be analyzed the operating ranges in which such effect results in significant changes in bearing behavior, in order to influence the dynamic rotor behavior.

2. METHODOLOGY

2.1 Lubrication models

The mathematical modeling that allowed the inclusion of the lubrication effect in the bearing's analysis was developed by Reynolds (1886), which in his work used the Navier-Stokes equations and continuity equation to determine the base equation of the classical theory of lubrication, described in Eq. 1.

$$\frac{\partial}{\partial x}\left(h^3\frac{\partial p}{\partial x}\right)+\frac{\partial}{\partial y}\left(h^3\frac{\partial p}{\partial y}\right)=6\mu\Omega R\frac{\partial h}{\partial x}+12\mu\frac{\partial h}{\partial t} \tag{1}$$

In this equation, μ indicates the absolute viscosity of the lubricating fluid, h is the film thickness, p is the hydrodynamic pressure developed on the bearing, Ω is the rotational speed of the shaft, R is the shaft's radius, and (x, y) are the circumferential and axial coordinates, respectively. The solution of the Reynolds equation allows the determination of the pressure distribution on the bearing, which is used to calculate the hydrodynamic forces.

The usual simulations for hydrodynamic bearings are directly performed from the Eq. 1 considering the Gümbell cavitation condition. This condition represents a simplistic approach since it does not treat the cavitation effect, it only supposes a zero pressure condition in the cavitation region. As proposed by Elrod (1981), the inclusion of the cavitation effect in the model is done by modifying the Reynolds equation with a dimensionless variable Θ which represents the ratio of the density of the fluid in a certain region with the density at the cavitation pressure $\left(\Theta=\frac{\rho}{\rho_c}\right)$. Another modification made in relation to the classical equation was the inclusion of a switch function g which assumes $g=1$ when the fluid is in a complete film region, or $g=0$ when the fluid is in a cavitation region. The use of this new variable in the Reynolds equation allied to the switch g function change the Eq. 1 to become the Eq. 2:

$$\frac{\partial\left(\rho_c\Theta h\right)}{\partial t}+\frac{\partial}{\partial x}\left(\frac{\rho_c\Theta hU}{2}-\frac{\rho_c\beta h^3 g}{12\mu}\frac{\partial\Theta}{\partial x}\right)+\frac{\partial}{\partial y}\left(-\frac{\rho_c\beta h^3 g}{12\mu}\frac{\partial\Theta}{\partial y}\right)=0 \tag{2}$$

In Eq. 2, β is the bulk modulus of the lubricating fluid and ρ_c is the density of the fluid in the cavitation region. It is important to note that the change in the Reynolds equation no longer allows the pressure to be calculated explicitly so, for this case, the pressure is implicitly calculated from the variable Θ, as shown in the Eq. 3 (Vijayaraghavan and Keith Jr, 1989).

$$p=p_{cav}+g\beta\ln\Theta \tag{3}$$

In this equation, p_{cav} is the cavitation pressure of the analyzed fluid.

There is no analytical solution for the Eq. 1 and Eq. 2 when considered bearings of finite length, so it becomes necessary to use a computational method capable to obtain the numerical solution for this type of problem. The Finite Volume Method (FVM) is considered as a good method of resolution because it's recommended for this type of geometry and conditions of the problem. In this work, the solution of the Eq. 2, which considers the effects of cavitation, is presented more explicitly. The solution of the Eq. 1 is more usual in the literature.

The solution of the Eq. 2 can be done dividing the modified Reynolds equation into four terms in order to simplify the equation.

$$\underbrace{\frac{\partial\left(\rho_c\Theta h\right)}{\partial t}}_{\text{IV}}+\underbrace{\frac{\partial}{\partial x}\left(\frac{\rho_c\Theta hU}{2}\right)}_{\text{I}}=\underbrace{\frac{\partial}{\partial x}\left(\frac{\rho_c\beta h^3 g}{12\mu}\frac{\partial\Theta}{\partial x}\right)}_{\text{II}}+\underbrace{\frac{\partial}{\partial y}\left(\frac{\rho_c\beta h^3 g}{12\mu}\frac{\partial\Theta}{\partial y}\right)}_{\text{III}} \tag{4}$$

The simulations developed for bearings assume two main solutions: solution for static loading and solution for dynamic loading. The solution for static loading neglects the term IV of the Eq. 4, since $\frac{\partial h}{\partial t}=0$. Thus, by integrating the terms I to III and adding them up, a system of linear equations can be obtained where the pressure of a volume of interest (Θ_P) depends on the other neighbors ($\Theta_E, \Theta_W, \Theta_N, and\ \Theta_S$), as verified in Eq. 5.

$$\Theta_P C_P=\Theta_E C_E+\Theta_W C_W+\Theta_N C_N+\Theta_S C_S \tag{5}$$

$$C_E=C_{2E}-C_{1E}h_E=-\frac{\beta\Delta y}{12\mu}\frac{h^3_{i+1/2}g_{i+1/2}}{\Delta x}-\left[1-\left(1-g_{i+1/2}\right)\right]\frac{\Omega R}{4}\Delta y\,h_E;$$

$$C_W=C_{2W}-C_{1W}h_W=-\frac{\beta\Delta y}{12\mu}\frac{h^3_{i-1/2}g_{i-1/2}}{\Delta x}-\left[-1-\left(1-g_{i-1/2}\right)\right]\frac{\Omega R}{4}\Delta y\,h_W;$$

$$C_N=-\frac{\beta\Delta x}{12\mu}\frac{h^3_{j+1/2}g_{j+1/2}}{\Delta y};$$

$$C_S=-\frac{\beta\Delta x}{12\mu}\frac{h^3_{j-1/2}g_{j-1/2}}{\Delta y};$$

$$C_P=(C_{2E}+C_{2W})+C_S+C_N-(C_{1E}+C_{1W})h_P$$

For the case of dynamic loading, the term IV is not neglected. The expression obtained by this approach can be seen in Eq. 6.

$$\Theta_P^t = \frac{\frac{\Omega}{\Delta x\ \Delta y}\left(\Theta_E^t C_E + \Theta_W^t C_W + \Theta_N^t C_N + \Theta_S^t C_S\right) - \frac{h_P \Theta^{t-\Delta t}}{\Delta t}}{-\frac{h_P}{\Delta t} - \frac{\partial h}{\partial t} + \frac{\Omega}{\Delta x\ \Delta y} C_P} \tag{6}$$

It is known that the equations obtained from the integration of the volume along its domain are valid for all elements individually, so, each one has a linear equation that describes the behavior of the fluid in its volume. Assembling all the equations, a system of linear equations is obtained, and its solution determines the pressure distribution on the bearing. The pressure distribution is used to determine the hydrodynamic forces on the bearing from the Eq. 7, thus leading to the inclusion of the lubrication effect in the rotor.

$$F_{Hidro} = \int_A p\, dA \tag{7}$$

2.2 Rotor Model

For this work, a rotor-bearings system is proposed for the computational simulations, in which the shaft elements (Bernoulli's beam), disc elements and bearings are considered. Figure 1 presents a typical system with these elements presented.

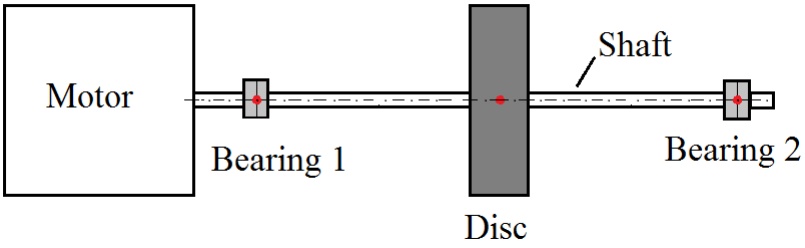

Figure 1: Example of setting of a rotating machine

One of the most used methods to model rotors is the Finite Element Method (FEM), responsible for discretizing the global domain of the rotor in a finite number of elements considered continuous in their local domain. The interaction between each one of the rotor elements is represented by the mass, stiffness, gyroscopic and damping matrices, which determine the distribution of these properties along the degrees of freedom of the system.

The determination of the global matrices aims to allow the obtainment of the equation of motion of the system, indicated in Eq. 8. This equation represents a system of nonlinear differential equations whose solution determines the dynamic behavior of the rotor.

$$[M]\left\{\ddot{q}\left(t\right)\right\} + \left(\left[C\right] + \Omega\left[G\right]\right)\left\{\dot{q}\left(t\right)\right\} + \left[K\right]\left\{q\left(t\right)\right\} = \left\{F\left(q, \dot{q}, t\right)\right\} \tag{8}$$

Where $[M]$, $[C]$, $[G]$ and $[K]$ are the global mass, damping, gyroscopic and stiffness matrices, respectively; $\{q\}$ is the degrees of freedom vector,$\{F\}$ is the excitation vector and Ω is the angular velocity of the rotor.

The equation of motion is obtained by assembling the global rotor matrices, as indicated by Nelson and McVaugh (1976), and determining the forces presents in the system. For this work was included the effect of the weight force, unbalance force of the shaft and hydrodynamic forces of the bearing. The weight force can be calculated from the system parameters and does not vary with time. The unbalance forces is a function of time and can be calculated from the Eq. 9.

$$\{F_D\} = \Omega^2 \eta \xi \begin{Bmatrix} \cos\left(\Omega t + \varphi\right) \\ \sin\left(\Omega t + \varphi\right) \\ 0 \\ 0 \end{Bmatrix} \tag{9}$$

In Eq. 9, η is the unbalanced mass, ξ is the unbalance eccentricity, and φ is the unbalance phase.

Finally, the hydrodynamic forces are a function of the position and speed of the rotor, consequently, a function of time. The calculation of this force is made from the determination of the pressure distribution previously presented.

The obtainment of the equation of motion allows advancing in the problem with the determination of the system response in the time. This part of the analysis must be done from a numerical integrator, capable of evaluating the forces at each instant of time and searching for the positions, velocities and nodal accelerations that lead to the solution of the equation of motion. In this work the integrator of Newmark is used because it is an implicit integrator indicated for the solution of non-linear problems.

3. RESULTS AND DISCUSSION

In order to verify the influence of cavitation on rotor's dynamic behavior, the numerical simulations were divided into two different loading conditions: static and dynamic loads. The simulation under static load seeks to verify if the inclusion of the cavitation effect in the bearing imply changes in the rotor's locus, while the simulation under dynamic load seeks to verify if the inclusion of the cavitation effect leads to changes in the rotor's response in the time and frequency domain. The system used in the simulations is shown in Fig. 2.

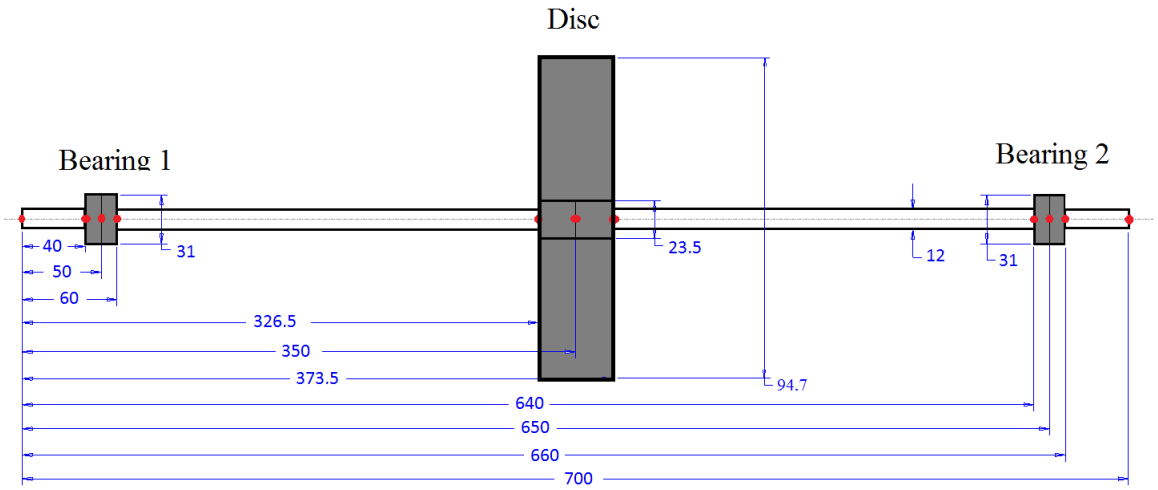

Figure 2: Sketch of the rotor (in mm)

The red dots of the Fig. 2 indicate the nodes of the elements used for FEM analysis. The rotor is symmetrically supported by bearings at its ends, whose properties can be seen in the Tab. 1. The material considered for both the shaft and the disc was steel ($E = 200\ GPa$, $\rho = 7850\ kg/m^3$ and $\nu = 0.3$).

Table 1: Bearing's and lubricant's properties used in simulation

Parameter and Units	**Symbol**	**Value**
Diameter [mm]	d	31
Length [mm]	l	20
Radial clearance [μm]	C_r	90
Absolut viscosity [Pa.s]	μ	0.05
Bulk modulus [GPa]	β	1.8

The size of the computational mesh for the analysis of the bearing was chosen after convergence tests, being considered 80 volumes in the circumferential direction (x) and 40 in the axial direction (y).

3.1 Static load

The first numerical simulation performed is related to static load. For this type of analysis, the locus of the shaft in the bearing is investigated considering the two different models of lubrication. The locus curve indicates, for a given static load, the shaft's positions on the bearing for different rotational speed. The load used for the simulation was 30 N, and the results obtained can be seen in the Fig. 3.

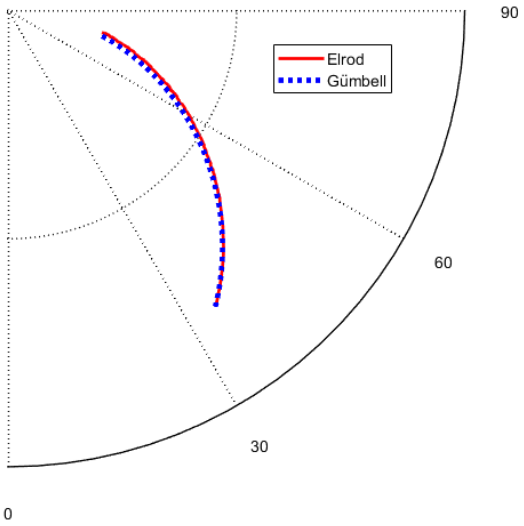

Figure 3: Results for simulation under static load

The Fig. 3 shows that there are no significant differences in the locus when considering the different models of lubrication. This shows that for static loading conditions, the inclusion of cavitation effects in bearing analysis does not imply significant changes on pressure distribution and hydrodynamic forces. This characteristic had already been discussed by Santos (1995), which performed the analysis for constant loading considering four different models of lubrication and found that the equilibrium position obtained for each of them was not significantly altered.

3.2 Dynamic load

The second numerical simulation was done considering the dynamic loading conditions. This characteristic of the system was given considering the operation of the rotor, which exerts a dynamic loading on the bearing due to its unbalance force. The purpose of this analysis is to verify if the change in the lubrication model would lead to changes in the rotor's response for different speeds of rotation.

The rotation speeds chosen for the analysis were: 10 Hz (normal operation), 22.5 Hz (natural frequency), 30 Hz (normal operation above natural frequency), 42 Hz and 43 Hz (close to instability). It is important to point out that the results presented refer to the orbit in steady-state response. To achieve this state, a simulation time of 10 seconds was required for the rotation speeds of 10, 22.5 and 30 Hz, while for the speeds of 42 and 43 Hz it took 20 seconds of simulation. For the analysis in frequency domain, the FFT is performed in the rotor's responses considering the variations of the signal in relation to the equilibrium position, i.e. the static gain is not evaluated (amplitude in zero frequency). The Fig. 4 to Fig. 8 show the results obtained for the dynamic case considering the rotor operation.

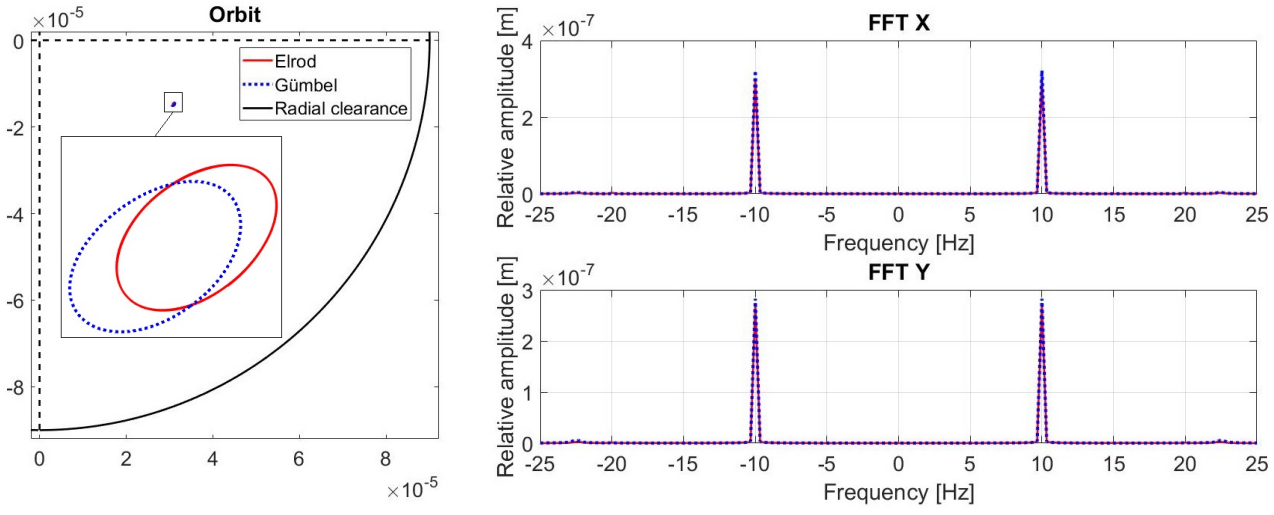

(a) Orbit to 10Hz

(b) FFT to 10Hz

Figure 4: Results obtained for 10Hz rotation speed

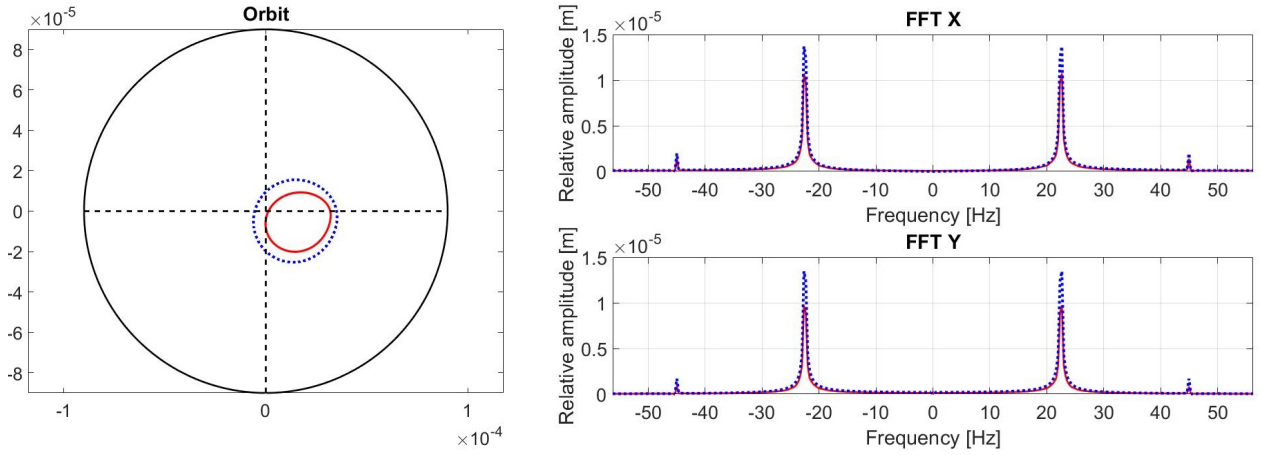

(a) Orbit to 22.5Hz (b) FFT to 22.5Hz

Figure 5: Results obtained for 22.5Hz rotation speed

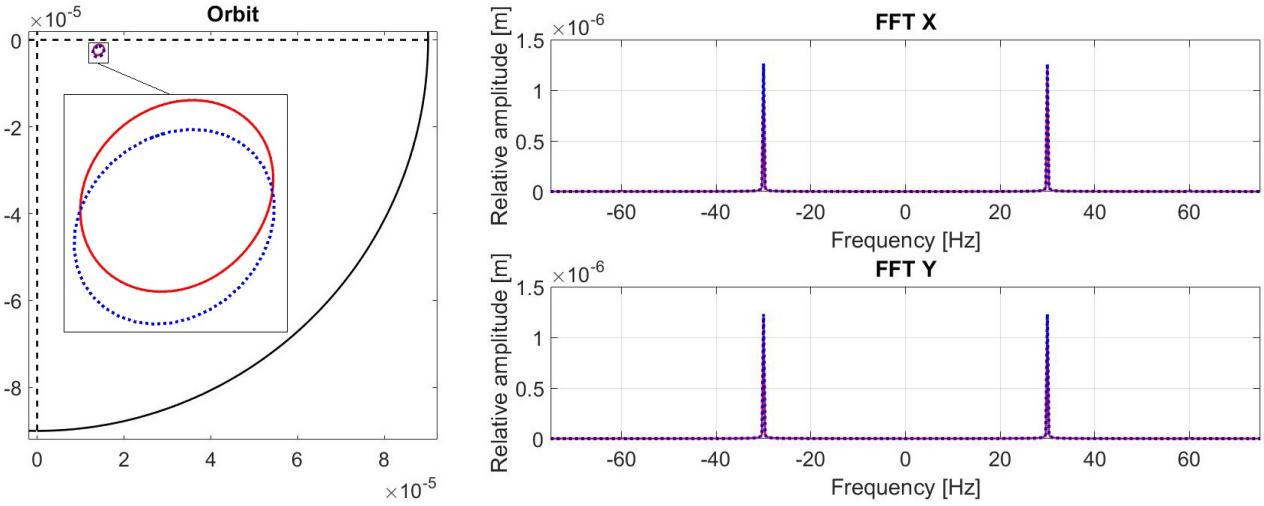

(a) Orbit to 30Hz (b) FFT to 30Hz

Figure 6: Results obtained for 30Hz rotation speed

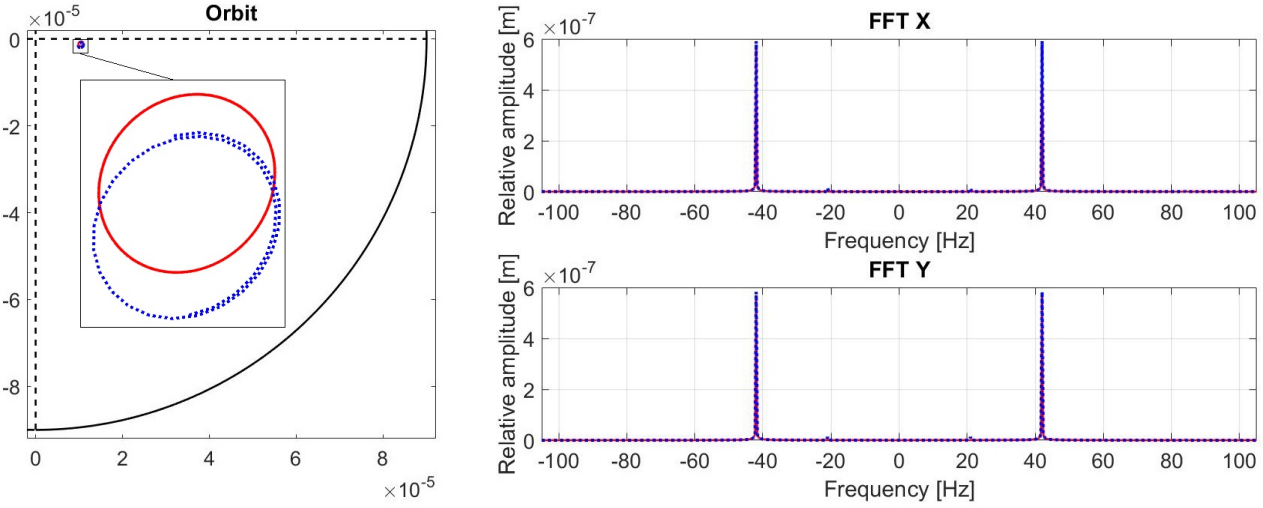

(a) Orbit to 42Hz (b) FFT to 42Hz

Figure 7: Results obtained for 42Hz rotation speed

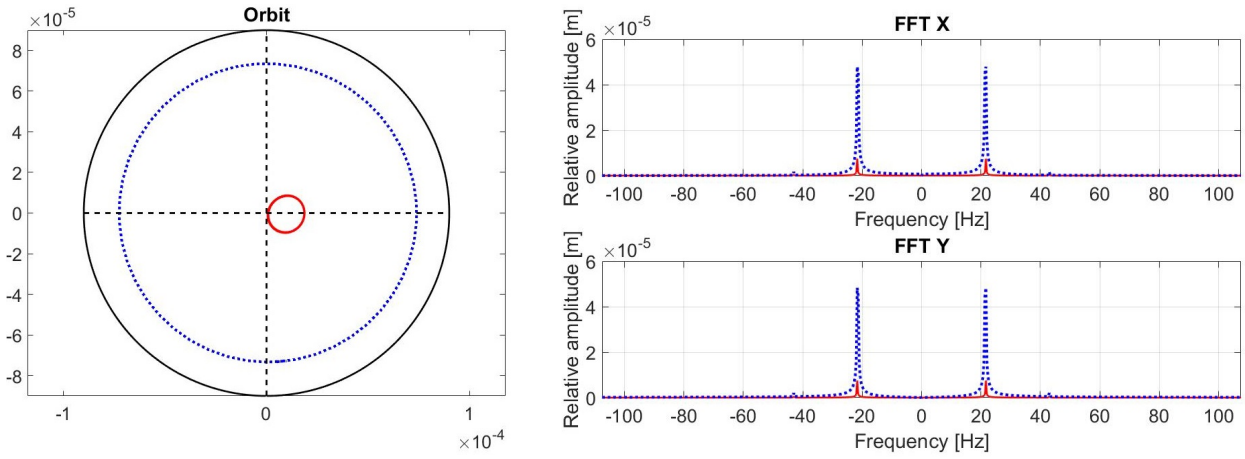

(a) Orbit to 43Hz

(b) FFT to 43Hz

Figure 8: Results obtained for 43Hz rotation speed

For the dynamic loading case, it is possible to observe that the lubrication model can lead to significant differences in the rotor's responses. According to Fig. 4a and Fig. 6a, the cases of 10 and 30 Hz do not present significant differences when observed globally, not leading to significant changes in the analysis of the rotor. Another important result in these cases is related to the FFT curves (Fig. 4b and Fig. 6b) which showed no difference between the peak position to the excitation's frequency, as well as the amplitude of both curves is close.

For the case of 42 Hz (Fig. 7a) it was possible to observe the same behavior observed for the cases of 10 and 30 Hz. However, a point to be highlighted is related to the FFT curve (Fig. 7b), where it is possible to check the second peak at half the excitation frequency for the model with the condition of Gümbell, while the same peak does not appear significantly for the Elrod condition model. Thus, the Elrod condition model tends to minimize the whirl effect in the rotor response.

To the 22.5 and 43 Hz cases, the differences are more visible and significant, even in relation to the overall view of the radial clearance. For the case of 22.5 Hz (Fig. 5a) it is possible to verify that the orbit of the model considering the effects of cavitation is smaller than the orbit of the model that does not consider. This fact may also be observed from the FFT of the signal (Fig. 5b)due to significant differences in peak amplitude. For the case of 43 Hz this difference is even more relevant since the difference between the orbits is even greater.

From these results, it was possible to verify that the inclusion of cavitation effects in the analysis of the bearing can lead to changes in the dynamic behavior of the rotor. This difference may not be significant, as observed for the 10 Hz, 30 Hz and 42 Hz cases. However, for some operational conditions this difference may become significant, such as shown under the natural frequency and close to the instability threshold.

4. CONCLUSION

This study aimed to verify if the inclusion of cavitation effects in the bearing lubrication model leads to significant changes in the rotor response when considered static and dynamic loading. Computational simulations were performed under static loading in order to analyze the shaft's locus. For the dynamic loading case, computational simulations were accomplished in order to analyze the rotor's response in time and frequency domain.

The analyzes accomplished in this work allow concluding that the cavitation effects do not lead to significant changes in the rotor behavior for the static case. However, for the dynamic case, it was possible to observe that the cavitation effects can influence the dynamic response of the rotor. For this reason, more studies should be performed in order to explore other ranges of operation and to identify at which of them the cavitation effect becomes relevant to the analysis.

From this analysis, this work contends that the inclusion of the cavitation effect on the bearing can lead to significant differences in the rotor response, however, this difference becomes significant in some operational conditions.

5. ACKNOWLEDGEMENTS

The authors would like to acknowledge the grants 2016/20975-4 and 2015/20363-6, São Paulo Research Foundation (FAPESP).

6. REFERENCES

Dowson, D. and Taylor, C., 1979. "Cavitation in bearings". *Annual Review of Fluid Mechanics*, Vol. 11, No. 1, pp. 35–65.

Elrod, H.G., 1981. "A cavitation algorithm". *Journal of Lubrication Technology*, Vol. 103, No. 3, pp. 350–354.

Floberg, L., 1974. "Cavitation boundary conditions with regard to the number of streamers and tensile strength of the liquid". *Cavitation and related phenomena in lubrication*, pp. 31–36.

Floberg, L., 1973. *On journal bearing lubrication considering the tensile strength of the liquid lubricant*. Lund Technical University.

Jakobsson, B. and Floberg, L., 1957. *The finite journal bearing, considering vaporization*. Gumperts Förlag.

Nelson, H. and McVaugh, J., 1976. "The dynamics of rotor-bearing systems using finite elements". *Journal of Engineering for Industry*, Vol. 98, No. 2, pp. 593–600.

Olsson, K.O., 1965. *Cavitation in dynamically loaded bearings*. Scandinavian Univ. Books.

Reynolds, O., 1886. "On the theory of lubrication and its application to mr. beauchamp tower's experiments, including an experimental determination of the viscosity of olive oil." *Proceedings of the Royal Society of London*, Vol. 40, No. 242-245, pp. 191–203.

Santos, E., 1995. *Carregamento dinamico de mancais radiais com cavitação do filme de oleo*. Ph.D. thesis, Universidade Federal de Santa Catarina, Centro Tecnologico.

Vijayaraghavan, D. and Keith Jr, T., 1989. "Development and evaluation of a cavitation algorithm". *Tribology Transactions*, Vol. 32, No. 2, pp. 225–233.

7. RESPONSIBILITY NOTICE

The authors are the only responsible for the printed material included in this paper.